# Lyapunov-based Integrator Resetting with Application to Marine Thruster Control

Jostein Bakkeheim, Tor A. Johansen, Øyvind N. Smogeli, and Asgeir J. Sørensen

***Abstract*—This paper addresses the idea of improving transient behavior by internal state resetting of dynamic controllers, such as controllers with integral action or adaptation. The concept presented here assumes that for a given closed loop system with a dynamic controller, improved transient performance is achieved when reset of controller states gives negative jumps in the Lyapunov function value. The Lyapunov function constitutes a part of the controller algorithm. By combining this with existing stability theory for switched systems, the stability analysis of the overall system follows directly. The framework assumes that a Lyapunov function is given, and that full state measurement is available for feedback. Moreover, an estimator is needed to give a coarse estimate of the system equilibrium point.**

**An anti-spin feature in local thruster speed control on ships with electric propulsion is in this paper presented as an application for the given framework. Transients arise when the ship operates in extreme seas, where disturbances such as ventilation and in-and-out of water effects may give rise to loss in propeller thrust. A Lyapunov function is used to decide appropriate reset of the integrator state of a standard PI-controller. The method is illustrated with experimental results.**

## I. Introduction

THE idea of resetting controller states was proposed by Clegg in 1958 [1], and resumed in the 1970's, see [2] and [3]. A renewed interest of these systems came up in late 1990's, see [4] and the references therein. A common strategy for these controllers is that they reset the output of the controller to zero when the input is zero. This turns out to improve phase lag properties in control of linear plant systems.

A different approach is seen in so called Multiple Model Adaptive Control (MMAC) frameworks. MMAC was first introduced for linear systems [5]–[10]. Recently, MMAC ideas have been extended to nonlinear systems [11]–[18]. The different approaches reported above are typically distinguished either by type of adaptive controller under consideration, or by the resetting strategy and criterion applied. In [14] and [18] the reset criterion makes use of a Lyapunov function in order to decide when to reset some or all of the controller states, not necessarily to zero, but rather to a value that ensures a negative drop in the Lyapunov function value. This may improve the overall transient performance of an adaptive control system. [14] presents an MMAC in an adaptive backstepping control algorithm. [17] is an extension of [14], discussing the effect of estimating the steady state, and gives tuning guidelines for the controller. In [18], MMAC is developed for adaptive control of feedback linearizable systems.

J. Bakkeheim and T.A. Johansen are with the Department of Engineering Cybernetics, Norwegian University of Science and Technology, Trondheim

Ø.N. Smogeli and A.J. Sørensen are with the Department of Marine Technology, Norwegian University of Science and Technology, Trondheim

Switching logic in the above references is based on the use of multiple Lypaunov functions [19], which preserves stability while guaranteeing faster parameter convergence. In this paper, we present the idea of resetting controller states based on the Lyapunov function value, and include this into a common framework. We also discuss the effect of estimating the Lyapunov function value instead of having perfect knowledge of this.

The method is illustrated for a ship anti-spin thruster controller for electrically driven thrusters. The thrusters draw power from power buses where the power is supplied by generators driven by diesel engines or gas turbines. This way of generating and transferring power to thrusters is becoming the standard in advanced ship propulsion for offshore vessels, cruise vessels, navy ships and some advanced tankers. In many cases the local thruster controllers (LTC) are conventional PI-controllers, controlling the propeller shaft speed. The PI-controller may be tuned such that the performance is acceptable in both steady-state and transient regimes. The tighter the PI-controller is tuned, the better the controller will perform in transient regimes. This will in turn increase the sensitivity to noise and increase variations in torque, power and mechanical load, which is not beneficial while in steady-state operation in waves. In normal operation, there may be no need for high transient performance. When the ship is in extreme seas, however, the propeller may start to spin due to ventilation (air suction from the free surface) and in-and-out-of water effects. This, in turn, may lead to wear and tear of the ship's propulsion equipment and undesired transients on the power bus that may increase the risk of blackouts due to overloading of the generator sets, see [20].

An anti-spin controller may handle these phenomena, see [21]–[24]. The anti-spin controller in these references is based on a combined power/torque thruster controller. A similar approach is considered here, but instead the anti-spin controller is based on a standard shaft speed PI-controller, where the integrator value may be reset if appropriate. The advantage of such a reset approach is that only minor software updates are needed to upgrade prevailing installations. Experimental test results are included in order to justify the method, see also [25] for preliminary results.

The paper is organized as follows. A framework for Lyapunov-based reset of dynamic controllers is presented in Section II. An anti-spin thruster controller is in Section III given as an application of the presented framework, where experimental test results follows in Section IV. Section V gives a comparison of the present controller strategy with other advanced state-of-the-art solutions reported in [21]–[24].

Finally, the conclusions are given in Section VI.

## II. Lyapunov-based reset of dynamic controllers

This section presents a framework for Lyapunov-based reset of dynamic controllers.

### A. Plant

Consider the following plant model

$$\dot{\xi} = f(\xi, u, \theta) \tag{1}$$
$$y = h(\xi) \tag{2}$$

where $\xi \in \mathbb{R}^n$ is the plant state vector, $u \in \mathbb{R}^m$ is the control input and $\theta \in \mathbb{R}^p$ is some unknown but constant disturbance or plant parameter vector. The vector field $f(\cdot,\cdot,\cdot)$ may be nonlinear. $y \in \mathbb{R}^v$ is the plant output, where $h(\cdot)$ may be nonlinear. It is assumed that the state $\xi$ is available for feedback.

### B. Dynamic Controller

Let $y^*$ denote some desired control reference. The task of the controller is to control the error $y^* - y$ to zero, hence control the state $\xi$ to some desired steady state $\xi^*(\theta, y^*)$. This steady state depends on the known desired control reference, but it may also depend on the unknown parameter vector $\theta$. Since the plant model contains some unknown parameters in $\theta$, it is common to augment the system with a set of controller states

$$\dot{z} = g(\xi, z, y^*) \tag{3}$$

where $z \in \mathbb{R}^q$ may represent an estimate of the unknown constants in $\theta$, leading to (3) being a part of an adaptive controller. On the other hand, $z$ may represent integrator states in an integral action control algorithm, where $\theta$ represents a disturbance to be rejected.

In addition to the dynamics (3) the controller is assumed to take the form

$$u = \gamma(\xi, z, y^*) \tag{4}$$

leading to the closed loop system

$$\dot{\xi} = f(\xi, \gamma(\xi, z, y^*), \theta) \tag{5}$$
$$\dot{z} = g(\xi, z, y^*). \tag{6}$$

The design of the controller (3)-(4) may not be a trivial task because the closed-loop equation in (5) and (6) depends on the unknown parameters $\theta$ in addition to being nonlinear. However, the design of a stabilizing controller (3)-(4) is outside the scope of the present paper, and we simply assume it is available.

The main idea in this paper is to improve transient performance of the existing closed-loop control system in (5) and (6) by utilizing the fact that the states $z$ may be reset to a different value taken from a finite set of candidates $z_i \in \mathcal{H}$ at any time instant.

### C. Lyapunov function

The error states of the system is given by

$$x = \begin{bmatrix} \xi^*(\theta, y^*) - \xi \\ z^*(\theta, y^*) - z \end{bmatrix} \tag{7}$$

where $x \in \mathbb{R}^{n+w}$.

*Remark 1:* $z^*(\theta, y^*) = \theta$ in an adaptive control algorithm, and $z^*(\theta, y^*)$ is the integrator steady state value in an integral control strategy.

Assume $x = 0$ is an equilibrium of the closed loop system with certain stability properties, and $D \subset \mathbb{R}^{n+p}$ is a domain containing $x = 0$. Let $V : D \to \mathbb{R}$ be a continuously differentiable Lyapunov function for the closed loop system.

We know that for a controller (3)-(4) rendering the equilibrium $x = 0$ stable in some sense, there exists a Lyapunov function $V(x)$. Such a function may be hard to find. While convergence properties can be proven for classes of adaptive systems, asymptotic stability properties may be hard to establish. In some controller design procedures, for example adaptive backstepping design [26] and optimal control, the Lyapunov function is obtained for free during the controller design process. In Receding Horizon Control, the Lyapunov function value can be obtained by solving an optimization problem online at each sample, see [27]. In this paper, we assume that $V$ is known.

### D. Reset procedure

A reset procedure may reset the controller state $z(t)$ to a different value $z_i \in \mathcal{H}$ taken from a set of candidates $\mathcal{H}$. A reset at time $t$ is done by resetting the state $z(t^+) = z_i$, where $t^+$ denotes an infinitesimal time increment of $t$. Stability is preserved if this is performed only when it leads to a negative jump in the Lyapunov function, $V(x(t^+)) < V(x(t))$, see [19].

Assuming that a reset to a lower Lyapunov function value gives a more favorable transient response, a reset according to the description above will lead to a closed-loop system (5) and (6) with improved transient performance.

### E. Effect of estimating $V(x)$

The above reset procedure needs information of the current Lyapunov function value. This is in general not known, since $\theta$ in (7) may be unknown, even if the plant state $\xi$ is measured.

*1) Noise and uncertainty:* The reset procedure may use $V(\hat{x})$, where $\hat{x}$ is an estimate of $x$. The estimate $\hat{x}$ may be found directly, or indirectly by first estimating the unknown plant parameter $\theta$, i.e. $\hat{\theta}$. Note that in an adaptive control algorithm where $z$ acts as an estimate of the unknown parameter $\theta$, the estimate $\hat{\theta}$ will be different from $z$, with other properties. The speed of convergence of $\hat{\theta}$ is required to be faster than $z$. The more slowly varying state $z$ may be reset to a different value in order to increase the transient response. The fast and hence maybe noisy signal $\hat{\theta}$ gives a rough guideline for where the equilibrium point is located. It must be fast in order to make the reset act quickly after some abrupt change in disturbance parameter or set-point, otherwise there would be no improvements in transient performance. It may

be noisy, but since this signal is not continuously connected to the control output, the noise propagation is restricted to instants of resets. However, a simple methodology given in [14] suggests to introduce a negative threshold $\delta$ in order to reduce undesirable switching due to these issues, i.e. reset to $x(t^+)$ only if $V(x(t^+)) < V(x(t)) - \delta$. Appropriate choice in sparseness of reset candidates $z_i \in \mathcal{H}$ may also give reduction of undesirable switching. These issues are discussed in greater detail in [17]. Also note that the reset strategy above may lead to chattering effects, since the steady state position is not exactly known. Introduction of a short dwell time $\tau$ between each reset action will reduce this problem, see [28]

*2) Performance specifications:* Using this reset strategy, we may separate the performance of the controller into two regimes. While in steady state, with a suitable tuned reset algorithm, the controller state will not reset such that the performance is given by the closed loop system without reset. If a sudden change in parameter value or set-point value occurs, the reset algorithm will detect this as a positive jump in the Lyapunov function value through the fast estimate $\hat{\theta}$. The reset algorithm will take action against this by demanding an appropriate reset of the controller state $z$, hence giving improved transient performance.

## III. Anti-spin in marine thruster control

The control hierarchy of a marine thruster control system consists of a high-level controller giving commands to a thrust allocation algorithm, which in turn gives commanded thrust set-points to the different LTCs, see [29]. Examples of high-level controllers are dynamic positioning (DP) systems, joysticks and autopilots.

An illustration of a thruster shaft speed control system is given in Figure 1. From the high-level control module, the desired propeller thrust $T_d$ is given as an input to the controller. Further, a direct mapping transforms this into the desired shaft speed $\omega_d$. This is in turn fed into a set-point mapping, which may limit the value of the desired shaft speed to cope with possible events of ventilation, see [21]–[24] for more details. The main idea pursued in this paper is that the dynamic part of the LTC, i.e. the integrator state in the PI-controller, may be reset to a different value only when large control errors are measured. The control error is a result of a sudden change in set-point or a ventilation incident, leading to a change in system steady state value. The control error is measured with the aid of the estimated Lyapunov function value. The reset event may lead to the thruster approaching its new steady state value faster.

With reference to Figure 1, the different blocks, i.e., thruster model, PI-controller, thrust to propeller speed mapping, set-point mapping, integrator resetting, propeller load torque observer, and ventilation detection, are considered in the following.

### A. Thruster model

The rotational dynamics are described as in [30] p. 473 by a first-order dynamic model for the propeller and shaft

$$J\dot{\omega} = Q_c - Q_p(\frac{h}{R}, \omega) - K_\omega \omega \tag{8}$$

where $Q_c$ is the commanded torque, $J$ is the rotational inertia of the propeller (including hydrodynamic added mass, shaft, gears and motor), $K_\omega$ is a linear friction coefficient, $\omega$ is the angular speed of the propeller, and $Q_p$ is the propeller load torque. The load torque $Q_p$ is modelled as

$$Q_p(\frac{h}{R}, \omega) = f_Q(\cdot) = Q_n(\omega)\beta_Q(\frac{h}{R}, \frac{\omega}{\omega_{max}}) \tag{9}$$

where $h/R$ is the relative submergence of the propeller, with $R$ being the radius of the propeller, and $h$ the shaft submergence. The nominal torque is

$$Q_n(\omega) = \Phi \text{sgn}(\omega)\omega^2 \tag{10}$$

where $\Phi = (K_{Q0}\rho D^5)/(4\pi^2)$, $D$ is the propeller diameter, and $\rho$ is the density of water. $K_{Q0}$ is the nominal torque coefficient commonly used for DP and low speed manoeuvering operations, when the advance speed $V_a$ is low. Different nominal coefficients $K_{Q0}$ for positive and negative speed may be used. For notational simplicity, we consider only one nominal coefficient. For transit operations with higher $V_a$, other models for $K_Q$ can be established. $\beta_Q$ in (9) expresses the torque loss, which is the ratio of actual to nominal torque, where $\omega_{max}$ is a chosen maximum speed of the propeller. Figure 2(a) shows a typical shape of this torque loss coefficient, see [24] for more details.

Finally, the propeller thrust is modelled as

$$T_p = f_T(\cdot) = \frac{K_{T0}\rho D^4}{4\pi^2}\text{sgn}(\omega)\omega^2\beta_T(\frac{h}{R}, \frac{\omega}{\omega_{max}}) \tag{11}$$

where $\beta_T$ is a thrust loss coefficient related to $\beta_Q$. $K_{T0}$ is the nominal thrust coefficient, i.e. for $V_a = 0$. In transit where $V_a \neq 0$, an alternative thrust coefficient $K_T(V_a)$ could be used.

### B. PI-controller

The shaft speed is given by a PI-controller

$$Q_c = K_p\left(\omega^* - \omega\right) + z \tag{12}$$

where $K_p > 0$ is the proportional gain and the integrator state is

$$\dot{z} = K_I\left(\omega^* - \omega\right) \tag{13}$$

with $K_I = K_p/T_i$ and $T_i > 0$ the integral time constant. The complete closed loop system becomes

$$\begin{aligned} \dot{\omega} &= \frac{1}{J}\left(-K_p\omega + K_p\omega^* - K_\omega\omega - Q_p(\frac{h}{R}, \omega) + z\right) \\ \dot{z} &= -K_I\omega + K_I\omega^*. \end{aligned} \tag{14}$$

Assuming $h/R$ and $\omega^*$ are constant, we obtain steady state values for $z$, i.e.

$$z^* = K_\omega\omega^* + Q_p(\frac{h}{R}, \omega^*). \tag{15}$$

Based on the definition of the error variables $\tilde{\omega} = \omega^* - \omega$ and $\tilde{z} = z^* - z$, we have the following error dynamics

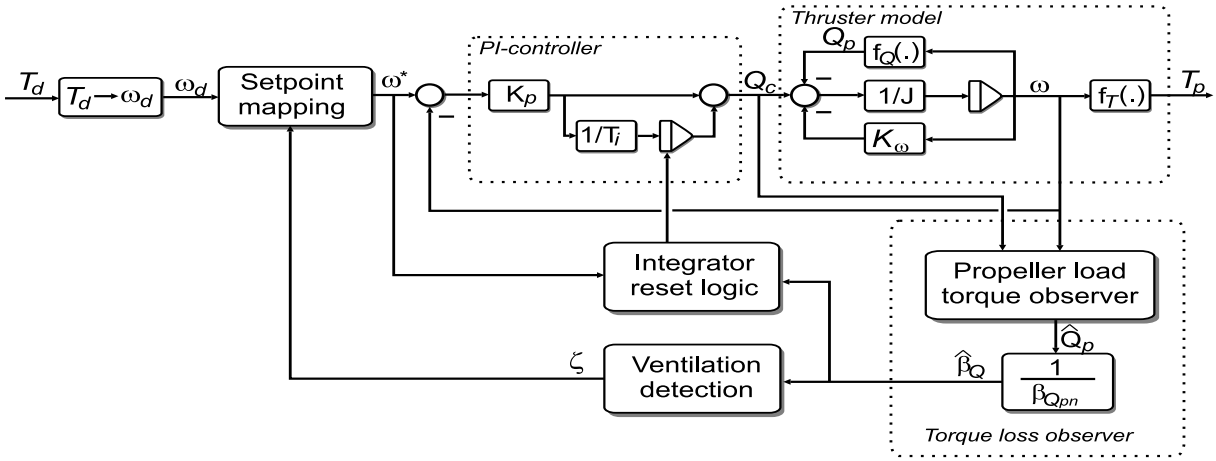


Fig. 1. Local thruster control system.

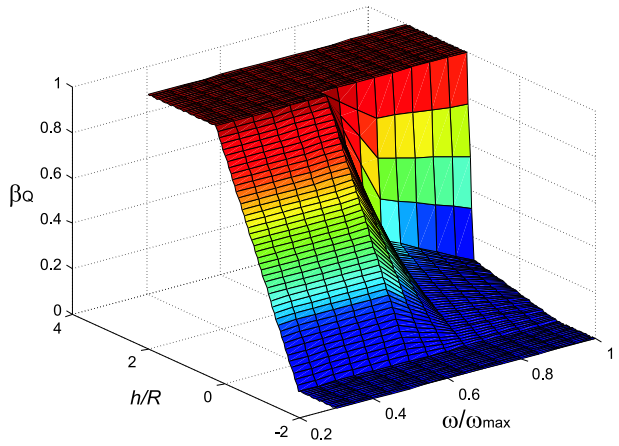


(a) Ventilation loss function $\beta_Q$.

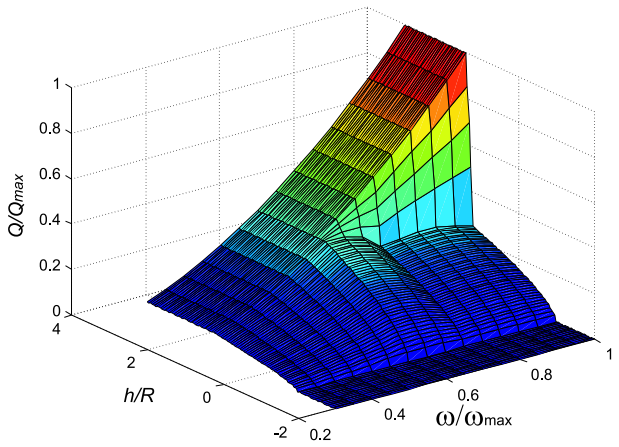


(b) Propeller load torque.

Fig. 2. Simulation model of ventilation loss and propeller load torque as functions of relative submergence $h/R$ and relative shaft speed $\omega/\omega_{max}$. These models are based on experimental results from a cavitation tunnel, see [24].

$$\dot{\tilde{\omega}} = \frac{1}{J}\left(\tilde{z} - (K_p + K_\omega)\,\tilde{\omega} + \left(Q_p(\frac{h}{R},\omega) - Q_p(\frac{h}{R},\omega^*)\right)\right) \tag{16}$$

$$\dot{\tilde{z}} = -K_I\tilde{\omega}.$$

Further defining $\tilde{x} = [\tilde{\omega},\, \tilde{z}]^T$, the control error may be written in compact form

$$\dot{\tilde{x}} = A\tilde{x} + \frac{1}{J}F(\tilde{x}, \frac{h}{R}, \omega^*) \tag{17}$$

where

$$A = \begin{bmatrix} -\frac{1}{J}\left(K_\omega + K_p - a\right) & \frac{1}{J} \\ -K_I & 0 \end{bmatrix} \tag{18}$$

$$F(\tilde{x}, \frac{h}{R}, \omega^*) = \begin{bmatrix} f\left(\frac{h}{R}, \omega^*, \tilde{\omega}\right) \\ 0 \end{bmatrix} \tag{19}$$

$$f(\frac{h}{R}, \omega^*, \tilde{\omega}) = Q_p(\frac{h}{R}, \omega^* - \tilde{\omega}) - Q_p(\frac{h}{R}, \omega^*) - a\tilde{\omega}. \tag{20}$$

The linear part $a\tilde{\omega}$ is subtracted from the nonlinearity in (16), leaving $F(\tilde{x}, \frac{h}{R}, \omega^*)$ as the remaining nonlinear part in (17). This is done in order to incorporate a linear approximation of the nonlinear part of the system as accurately as possible. The nonlinear system may then be approximated by a linear system when we search for a Lyapunov function, and analyze the effects of the nonlinearity later.

We know that for $A$ Hurwitz, there exists a solution $P^T = P > 0$ of the Lyapunov equation

$$A^T P + PA = -Q \tag{21}$$

where $Q^T = Q > 0$ and in general

$$P = \begin{bmatrix} p_{11} & p_{12} \\ p_{12} & p_{22} \end{bmatrix}. \tag{22}$$

The following choice of Lyapunov candidate

$$V(\tilde{x}) = \tilde{x}^T P \tilde{x} \tag{23}$$

will prove stability of the closed loop system.

*Proposition 1:* Assume $\omega^*$ and $h/R$ constant, and suppose $K_I$ and $K_p$ are chosen such that $A$ is Hurwitz and $P^T =$

$P > 0$ is a solution to the Lyapunov equation (21), where $Q = \text{diag}(q_{11}, q_{22}) > 0$. Further, if there exists an $\alpha$ such that the graph of $f(\frac{h}{R}, \omega^*, \tilde{\omega})$ is a function of $\tilde{\omega}$ inside sector $[-\alpha, \alpha]$, and there exist $\mu_1 > 0$ and $\mu_2 > 0$ such that

$$q_{11} - \frac{1}{J}(\mu_1 + \mu_2)\alpha^2 - \frac{1}{J\mu_1}(p_{11})^2 > 0 \tag{24}$$

$$q_{22} - \frac{1}{J\mu_2}(p_{12})^2 > 0 \tag{25}$$

holds, then the origin $\tilde{x} = 0$ is a globally exponentially stable (GES) equilibrium point of (17).

*Proof:* The time derivative of (23) along the trajectories of the nonlinear system (17) is

$$\dot{V}(\tilde{x}) = -\tilde{x}^T Q\tilde{x} + \frac{2}{J}\tilde{x}^T PF(\tilde{x}, \frac{h}{R}, \omega^*). \tag{26}$$

The two terms in (26) are

$$-\tilde{x}^T Q\tilde{x} = -q_{11}\tilde{\omega}^2 - q_{22}\tilde{z}^2 - 2q_{12}\tilde{\omega}\tilde{z} \tag{27}$$

and

$$\begin{aligned}\frac{2}{J}\tilde{x}^T PF(\tilde{x}, \frac{h}{R}, \omega^*) = \frac{2}{J}p_{11}\tilde{\omega}f(\frac{h}{R}, \omega^*, \tilde{\omega}) \\ + \frac{2}{J}p_{12}\tilde{z}f(\frac{h}{R}, \omega^*, \tilde{\omega}).\end{aligned} \tag{28}$$

Using Young's inequality, $2xy \leq \frac{1}{\mu}x^2 + \mu y^2, \quad \forall \mu > 0$, on the second term in (28), we obtain

$$\begin{aligned}\frac{2}{J}\tilde{x}^T PF(\tilde{x}, \frac{h}{R}, \omega^*) \leq \frac{1}{J\mu_1}(p_{11}\tilde{\omega})^2 + \frac{1}{J}\mu_1 f^2(\frac{h}{R}, \omega^*, \tilde{\omega}) \\ + \frac{1}{J\mu_2}(p_{12}\tilde{z})^2 + \frac{1}{J}\mu_2 f^2(\frac{h}{R}, \omega^*, \tilde{\omega}).\end{aligned} \tag{29}$$

Since $Q$ is diagonal and $f(\frac{h}{R}, \omega^*, \tilde{\omega})$ belongs to the sector $[-\alpha, \alpha]$, i.e. $f^2(\frac{h}{R}, \omega^*, \tilde{\omega}) \leq (\alpha\tilde{\omega})^2$, $\forall\tilde{\omega}$ for constant $\omega^*$ and $h/R$, we obtain

$$\begin{aligned}\dot{V}(\tilde{x}) \leq -\left(q_{11} - \frac{1}{J}(\mu_1 + \mu_2)\alpha^2 - \frac{1}{J\mu_1}(p_{11})^2\right)\tilde{\omega}^2 \\ - \left(q_{22} - \frac{1}{J\mu_2}(p_{12})^2\right)\tilde{z}^2 = -W(\tilde{x}).\end{aligned} \tag{30}$$

From (24)-(25), the function $W(\tilde{x})$ is positive definite, hence GES follows from Thm 4.1 in [31]. ■

### C. Thrust to propeller speed mapping

The industrial standard for fixed pitch propellers is shaft speed control based on a static mapping from desired thrust $T_d$ to desired shaft speed $\omega_d$, obtained by simply taking the inverse mapping of (11):

$$\omega_d = 2\pi\text{sgn}(T_d)\sqrt{\left|\frac{T_d}{K_{T0}\rho D^4}\right|}. \tag{31}$$

### D. Integrator resetting

For a sudden change in the loss factor $\beta_Q$ due to change in $h/R$, the Lyapunov function value may make a positive jump due to its new equilibrium point. Integrator reset may improve performance in transient regimes, when the equilibrium suddenly changes due to ventilation or set-point change, without influencing performance in steady-state.

To maintain stability when the integrator is reset, one may perform a reset only when this leads to a negative jump in the Lyapunov function. The following lemma states the jump value in the Lyapunov function (23) as a result of performing a reset of the integrator state.

*Lemma 1:* A reset of the integrator value $z(t^+)$ to $z_i$, where $t^+$ denotes an infinitely small time increment of $t$, of system (17) leads to a jump in the Lyapunov function (23)

$$\Delta V_i(t) = p_{22}\left(\tilde{z}_i^2 - \tilde{z}^2(t)\right) + 2p_{12}\tilde{\omega}(t)\left(\tilde{z}_i - \tilde{z}(t)\right) \tag{32}$$

where $\tilde{z}_i = z^* - z_i$.

*Proof:* Let $\tilde{\omega}_i = \omega^* - \omega_i$ and $\tilde{x}_i = [\tilde{\omega}_i,\ \tilde{z}_i]^T$. The jump in the Lyapunov function is calculated as

$$\begin{aligned}\Delta V_i(t) &= V(\tilde{x}_i) - V(\tilde{x}(t)) = \tilde{x}_i^T P\tilde{x}_i - \tilde{x}^T(t)P\tilde{x}(t) \\ &= p_{11}\tilde{\omega}_i^2 + p_{22}\tilde{z}_i^2 \ + 2p_{12}\tilde{\omega}_i\tilde{z}_i \\ &\quad - p_{11}\tilde{\omega}^2(t) - p_{22}\tilde{z}^2(t) \ - 2p_{12}\tilde{\omega}(t)\tilde{z}(t) \\ &= p_{22}\left(\tilde{z}_i^2 - \tilde{z}^2(t)\right) + 2p_{12}\tilde{\omega}(t)\left(\tilde{z}_i - \tilde{z}(t)\right)\end{aligned} \tag{33}$$

where the fact that $\tilde{\omega}_i = \tilde{\omega}(t)$, due to the continuity of solutions of ordinary differential equations, has been used. ■

We assume a finite set of integrator reset candidates, $\mathcal{H} = \{z_1, \ldots, z_n\}$. The following result states stability when the integrator is reset.

*Proposition 2:* Given the closed-loop system with PI-controller (17). Assume that $V$ in (23) is a Lyapunov function that proves the equilibrium point of the nonlinear system in (17) to be GES. Further assume that $\Delta V_i(t)$ denotes the jump in the Lyapunov function value if the integrator of the PI-controller in (17) is reset to a value $z_i \in \mathcal{H}$. Then if $z$ is reset to the value $z_i$ only if $\Delta V_i(t) < 0$, the equilibrium point of the nonlinear system in (17) is GES.

*Proof:* The reader is referred to [19], where the switching system is proved to be stable in the sense of Lyapunov if $\Delta V_i(t) < 0$. Further, the condition $\Delta V_i(t) < 0$ leads to a negative jump in the Lyapunov function, which also leads to $\dot{V}(\tilde{x}) \leq -W(\tilde{x})$ see (30), hence GES follows. ■

*Remark 2:* Assume the choice of $Q$ in (21) is made in such a way that the Lyapunov function is an appropriate measure of remaining transient energy. Then, in addition to the overall stability being preserved with resetting, there will be a transient performance improvement if the system is reset.

*Remark 3:* The results in Proposition 1 and 2 assume $\omega^*$ and $h/R$ being constant. Abrupt changes in the disturbance parameter $h/R$ or the set-point $\omega^*$ may lead to increases in the Lyapunov function value $V(x)$. The results above state that $V(x)$ will decay exponentially between each abrupt event, with improved transient behavior. In situations where periodic disturbances or changes in set-point lead to the overall performance not being GES, the overall performance is practically improved.

### E. Propeller load torque observer

Based on the rotational dynamics (8), the observer equations for the estimated propeller load torque $\hat{Q}_p$ presented in [32], [22], [23] and [24] are written

$$\begin{aligned}\dot{\hat{\omega}} &= \frac{1}{J}(-\hat{Q}_p - K_\omega\hat{\omega} + Q_c) + k_1(y - \hat{y}),\\ \dot{\hat{Q}}_p &= -k_2(y - \hat{y}),\end{aligned} \tag{34}$$

where the propeller load torque $Q_p$ has been modelled as a random process driven by a bounded noise, and the shaft speed $\omega$ is taken as the measured output $y$ (and hence $\hat{y} = \hat{\omega}$). The equilibrium point of the observer error dynamics is globally exponentially stable (GES) in the case of a constant load torque if the observer gains $k_1$ and $k_2$ are chosen according to

$$k_1 > -K_\omega/J, \quad k_2 < 0, \tag{35}$$

see [32] for more details.

An estimate of the torque loss factor $\beta_Q$ may be calculated based on the estimated propeller load torque $\hat{Q}_p$ from (34) and an estimated nominal load torque $\hat{Q}_n$. $\hat{Q}_n$ is given from (10) by feedback from the propeller shaft speed $\omega$ as

$$\hat{Q}_n(\omega) = \Phi\text{sgn}(\omega)\omega^2. \tag{36}$$

The estimated torque loss with respect to the nominal torque expected from the measured shaft speed is then

$$\hat{\beta}_Q = \alpha_b(\omega) + (1 - \alpha_b(\omega))\frac{\hat{Q}_p}{\hat{Q}_n}. \tag{37}$$

$\alpha_b(\omega)$ is a weighting function of the type

$$\alpha_b(y) = e^{-k|py|^r} \quad \text{for} \quad y \in \mathbb{R}, \tag{38}$$

where $k$, $p$ and $r$ are positive tuning gains. The weighting function is needed because the estimate otherwise would be singular for zero shaft speed [32].

### F. Ventilation detection

The estimated loss factor $\hat{\beta}_Q$ may be subject to some fluctuations during the period of ventilation. Instead of using this estimate directly as a measure of whether the propeller is ventilating or not, a translation of this value into a discrete value $\zeta$ may be appropriate, see [21]–[24]. For a single ventilation incident, $\zeta$ will have the following evolution:

$$\begin{aligned}&\hat{\beta}_Q \geq \beta_{v,on} \Rightarrow \zeta = 0 \quad \text{(no ventilation)}\\ &\hat{\beta}_Q < \beta_{v,on} \Rightarrow \zeta = 1 \quad \text{(ventilation)}\\ &\hat{\beta}_Q \geq \beta_{v,off} \Rightarrow \zeta = 0 \quad \text{(no ventilation).}\end{aligned} \tag{39}$$

$\beta_{v,on}$ and $\beta_{v,off}$ are thresholds for beginning and termination of ventilation. Note that the ventilation detection $\zeta$ includes hysteresis, hence robustness due to measurement noise in the loss value estimate $\hat{\beta}_Q$ is achieved.

### G. Effects of not knowing the loss factor

Because the loss factor $\beta_Q$ is unknown, the steady state value $z^*$ in (15) is estimated by

$$\hat{z}^* = K_\omega\omega^* + \Phi\text{sgn}(\omega^*)\omega^{*2}\hat{\beta}_Q \tag{40}$$

where the estimate of the loss factor $\hat{\beta}_Q$ is given in (37). Hence, the Lyapunov function value used in the integrator reset algorithm is also an estimate. Erroneous resets due to measurement noise during estimation of $z^*$ in (40) is reduced by decreasing the density of integrator reset candidates in $\mathcal{H}$ as discussed in Section II-E.

### H. Set-point mapping

In normal operation, increasing the rotational speed of the propeller leads to an increase in the propeller thrust and load torque. However, in case of ventilation, this may lead to increased dynamic loads, and hence mechanical wear and tear and power fluctuations, without increasing the thrust. In [24] both stationary and dynamical tests of these effects are studied. Due to the given controller design, and since the desired thrust $T_d$ is the input of the controller, a set-point mapping may prevent the controller from demanding torque above the limit of saturation. This will also reduce wear and tear of the propulsion device:

$$\omega^* = \begin{cases} \omega_{opt}, & \text{if } \zeta = 1 \text{ and } \omega_d \geq \omega_{opt} \\ \omega_d, & \text{otherwise} \end{cases} \tag{41}$$

where $\omega_{opt}$ is some optimal propeller speed during ventilation, $\omega_{opt}/\omega_{max} = 0.45$ in Figure 2(b).

## IV. Experimental test results

An experimental set-up in the Marine Cybernetics Laboratory (MCLab) at NTNU was used to test the resulting control strategy, see Figure 3. The thruster set-up had the following physical characteristics:

| $D$ | $J$ | $K_\omega$ | $K_{T0}$ | $K_{Q0}$ |
|---|---|---|---|---|
| 0.25 m | 0.005 kgms$^2$ | 0.01 Nms | 0.575 | 0.075 |

where the maximum speed of the propeller was $\omega_{max} = 125$ rad/s. The proportional gain and integral time constant of the controller were $K_p = 0.032$ and $T_i = 0.05$, respectively.

In this set-up, the thruster is stationed at a fixed horizontal position, centered in the basin. Hence, the use of the nominal thrust and torque coefficients $K_{T0}$ and $K_{Q0}$ in (31) and (10) are appropriate.

The nonlinear term $Q_p(\frac{h}{R}, \omega) - Q_p(\frac{h}{R}, \omega^*)$ in (20) is shown in Figure 4 for different values of $\omega^*$. The loss factor $\beta_Q$ is assumed to be constant equal to 1, where the nonlinear term is most dominant.

We consider $\tilde{\omega} \in [-125, 125]$, hence $a = -0.33$ will minimize the remaining nonlinear part $f(\frac{h}{R}, \omega^*, \tilde{\omega})$ enclosed inside the sector $[-\alpha, \alpha]$, see Figure 4. However, note that $f(\frac{h}{R}, \omega^*, \tilde{\omega})$ may not be enclosed inside the sector $[-\alpha, \alpha]$ for $|\tilde{\omega}| > 125$, but due to $\tilde{\omega} \in [-125, 125]$, exponential stability (ES) may still be ensured for all feasible initial conditions.

The resulting eigenvalues of the matrix $A$ in (18) are $\lambda_1 = -73.4$ and $\lambda_2 = -1.7$. Including the sector $\alpha = 0.37$ from

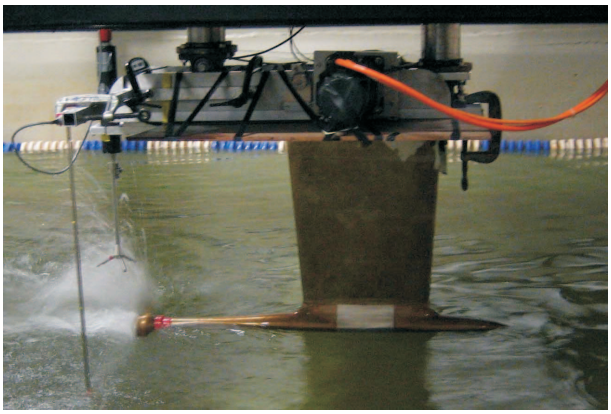

Fig. 3. A test set-up in MCLab at NTNU. The local thruster controller with integrator reset was tested in a basin. The thruster vertical position was moved in order to trigger ventilation and in-and-out-off water effects.

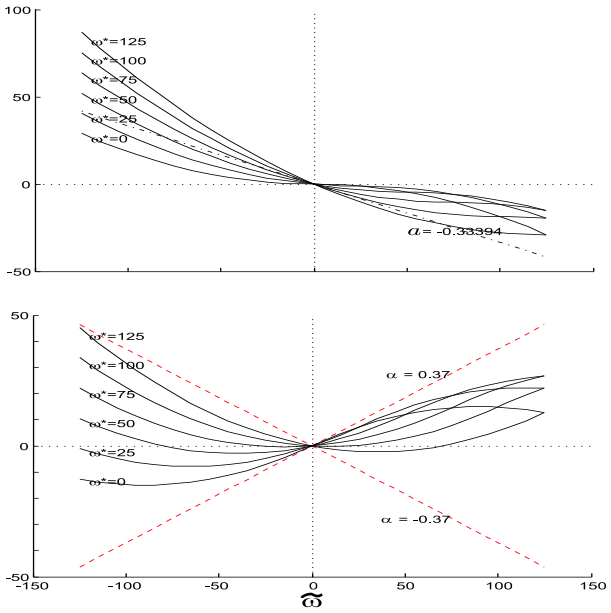


Fig. 4. **Upper:** Load torque nonlinearities $Q_p(\frac{h}{R},\omega) - Q_p(\frac{h}{R},\omega^*)$ in (20) for different values of $\omega^*$ running from $\tilde{\omega} = -125$ to $\tilde{\omega} = 125$ with $\beta_Q = 1$. The dotted line represents the linear part $-a\tilde{\omega}$ in (20). **Lower:** The minimized nonlinear term $f(\frac{h}{R},\omega^*,\tilde{\omega})$ in (20) for different values $\omega^*$ for $\tilde{\omega} \in [-125, 125]$ enclosed inside sector $[-\alpha, \alpha]$ for all feasible $\tilde{\omega}$.

Figure 4 in Lemma 1, ES of the nonlinear system (17) is proven with $Q = \text{diag}(1, 0.1)$, $\mu_1 = 0.015$ and $\mu_2 = 0.00012$. The solution of (21) is

$$P = \begin{bmatrix} 0.006652 & -2.5 \cdot 10^{-4} \\ -2.5 \cdot 10^{-4} & 2.1081 \end{bmatrix}, \tag{42}$$

hence (23) will act as a suitable Lyapunov function.

For evaluation of the modular integrator reset strategy outlined in this paper, test scenarios are given both with and without the reset module. With reference to Figure 2, the propeller speed region of interest is selected to be located above $\omega/\omega_{max} = 0.45$. The desired thrust was therefore chosen as $T_d = 300$ N which yields $\omega_d = 73$ rad/s. Tests were performed both with and without the set-point mapping. To demonstrate LTC in extreme seas, the propeller was moved in and out of the water by raising and lowering the thruster with a period of 5 seconds and an amplitude of 15 cm. The propeller was then fully submerged at its lower position, i.e. the distance from the propeller blades to the sea surface was 5 cm. In the upper position, the shaft of the propeller was in the mean free surface.

Plots of the experimental results are shown in Figures 5-8. A wave probe was used for measuring the relative submergence $h/R$. In order to plot the reset progress, $\sigma(t)$ is defined as

$$\sigma = \begin{cases} z_i, & \text{if } \Delta V_i < 0 \\ -1, & \text{otherwise} \end{cases}. \tag{43}$$

The exact Lyapunov function value is not available, but an estimate $\hat{V}$ is included in the plots. Thrust and torque sensors on propeller shaft were used to measure $T_p$ and $Q_p$. The motor time constant is neglected in this paper, supported by the agreement between commanded motor torque $Q_c$ and measured motor torque $Q_m$.

The controller was implemented in Simulink, where the real-time system Opal RT-Lab QNX was used to interface the Simulink environment to the motor drive and the sensors. A sampling period of $0.008s$ was used, where a search for a new reset candidate was attempted at all samples. In situations where more than one candidate satisfied the reset criterion, the one with largest drop in Lyapunov function value was selected.

Figure 5 shows a situation where a conventional PI-controller is used. Note the peaks in propeller speed $\omega$ when the propeller ventilates. Also note the positive jumps in the estimated Lyapunov value due to shifted equilibrium point when the propeller starts and stops ventilating. The same situation is shown in Figure 6, but with integrator resetting. Clearly, the reset leads to reduced peaks in $\omega$. The plots of $\hat{V}$ show the transient reductions when the PI-controller is reset. Also note that the mean propeller thrust $\bar{T}_p$ is increased when the PI-controller is reset: the mean propeller thrust without reset is $\bar{T}_p = 136$ N while the value with reset is $\bar{T}_p = 152$ N.

Figures 7 and 8 show the same controllers as Figures 5 and 6, but with a set-point mapping to $\omega^* = 56$ when ventilation is detected. Note the peak reduction of $\omega$ in Figure 8, where the integrator resetting is made active. In this last situation, a positive slew rate limiter has been included at the integrator output. This reduces the noise in the estimated $\hat{\beta}_Q$, and hence reduces the risk of performing erroneous resets. A more sophisticated solution to this issue would be to implement the noise reduction in the estimator $\hat{\beta}_Q$ instead. This is not considered here. A brief discussion of this problem is included in [32]. The mean propeller thrust is in this case kept more or less constant with the introduction of integrator reset: $\bar{T}_p = 130$ N without reset, while $\bar{T}_p = 128$ N with reset. The small reduction may be due to the introduction of the slew rate limiter. A more appropriate choice of this slew rate limiter may lead to an increase rather than a decrease of the thrust.

## V. Discussion

The anti-spin strategies in [21]–[24] and the present paper are all based on the same observer, set-point mapping and

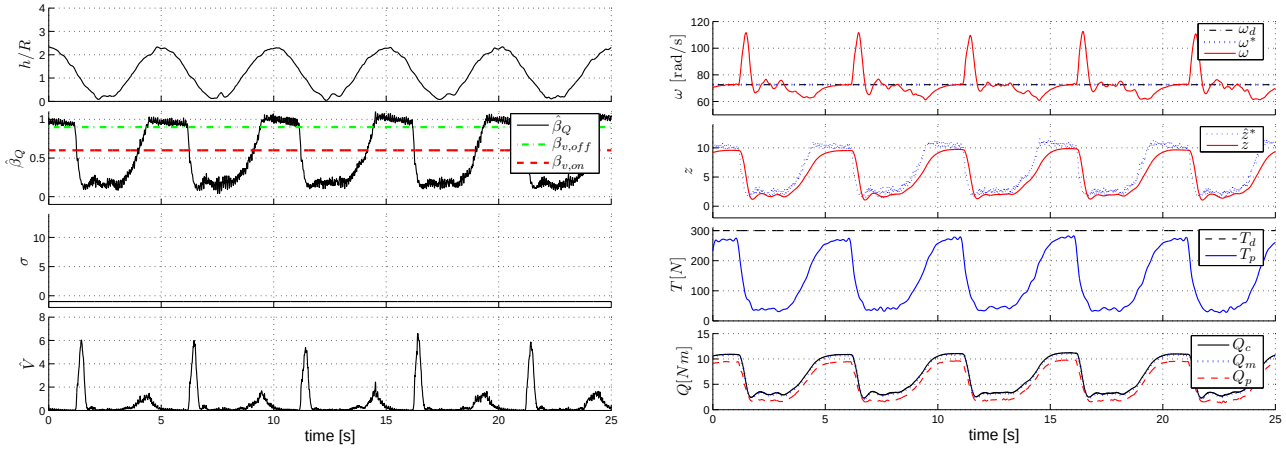


(a) (b)

Fig. 5. Experimental results with local thruster PI-control (no reset). Desired speed $\omega_d = 73$.

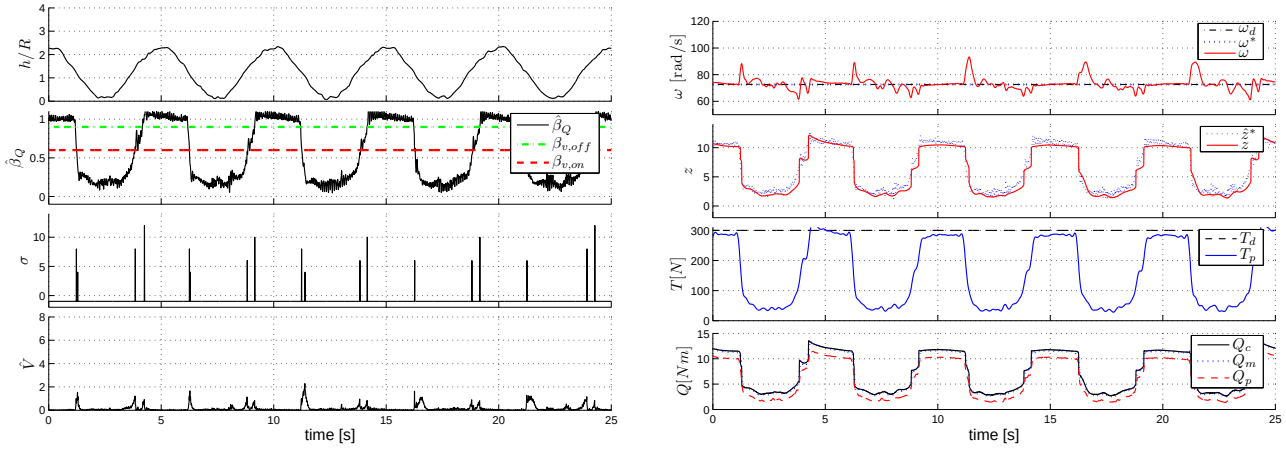


(a) (b)

Fig. 6. Experimental results of the same situation as in Figure 5, but with integrator resetting with the following candidates: $\mathcal{H} = \{0,\ 2,\ 4,\ 6,\ 8,\ 10,\ 12\}$.

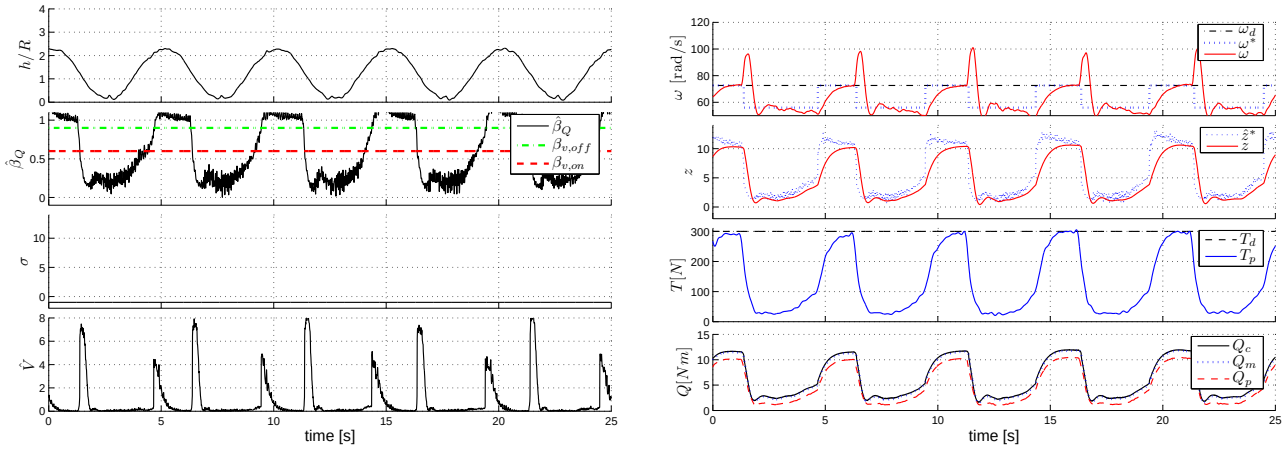


(a) (b)

Fig. 7. Experimental results with local thruster PI-control and set-point mapping (no reset). When ventilation is detected, the set-point of the PI-controller is changed from the initial $\omega_d = 73$, to a lower value $\omega^* = 56$.

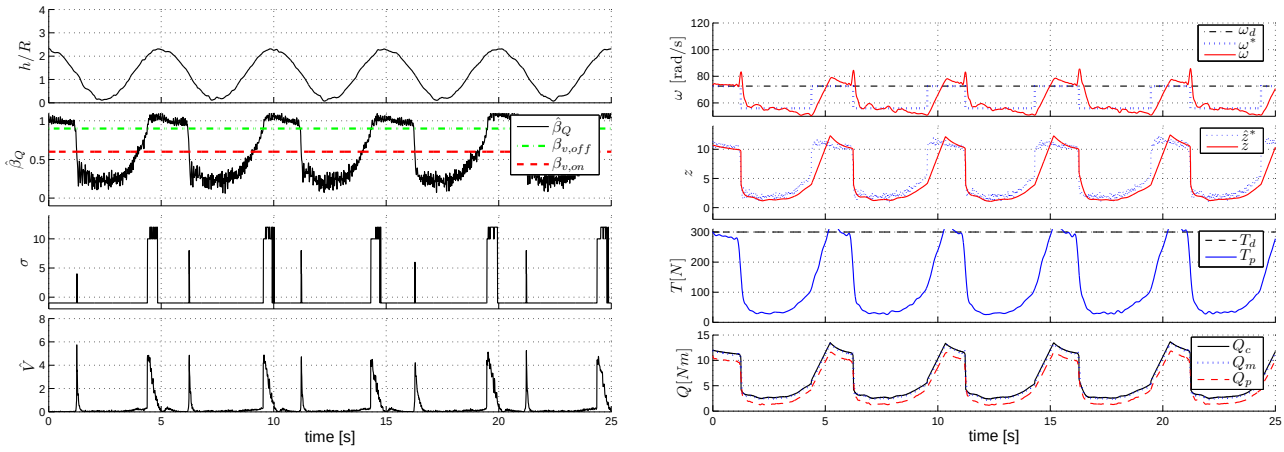


(a) (b)

Fig. 8. Experimental results of the same situation as in Figure 7, but with integrator resetting with the following candidates: $\mathcal{H} = \{0, 2, 4, 6, 8, 10, 12\}$.

detection algorithm, deviating only by selection of parameter values. However, the core controllers, i.e. the controllers used in normal conditions, are not the same. In [21]–[24] the core controller is a combined torque/power controller, and in the present paper the core controller is a regular shaft speed PI-controller. In [21] and [23], the output of the controller is modified by a dynamic scaling factor to give a nearly constant shaft speed when ventilation is detected.

In [22], however, a switch to a speed-controller is made when ventilation is detected. The PI-controller is in this case not equipped with integrator resetting, but the controller may be tuned tighter compared to a PI-controller for normal conditions. A comparison of the strategies presented in [21]–[23] is given in [24]. By appropriately tuning the different strategies, no or little deviation in performance is experienced. This is also the case when comparing the solutions in [21]–[24] with the present one. They all solve the problem of anti-spin in more or less the same way regarding performance, but separate in the way of doing this - the main performance difference lies in the choice of basic controller. The present strategy has an advantage in terms of implementation in that it only needs tuning of the reset algorithm as a separate module. The parameters of the shaft speed PI-controller module are already tuned.

## VI. Conclusion

We have presented a framework for reset control, generalizing existing methods where a Lyapunov function is used as a design tool in order to improve transient performance of systems with dynamic controllers. The method in the framework is based on resetting controller states to different values when this leads to a negative jump in the Lyapunov function.

This method has been applied on a PI-controller for marine thruster speed control by integrator resetting in order to improve the transient performance of the local thruster controller.

A test of the control strategy was made in a basin, where improved performance is observed at situations where the propeller ventilates. Tests showed reduced peaks in propeller speed, hence reduction of structural loads on propeller blades, while maintaining or even increasing the mean propeller thrust.

## Acknowledgment

This work was in part sponsored by the Research Council of Norway, project number 157805/V30.

## References

[1] J. C. Clegg, "A Nonlinear Integrator for Servomechanisms," *Trans. A.I.E.E.*, vol. 77 (Part II), pp. 41–42, 1958.

[2] K. R. Krishnan and I. M. Morowitz, "Synthesis of a Non-linear Feedback System with Significant Plant-ignorance for Prescribed System Tolerance," *Int. J. Contr.*, vol. 19, pp. 689–706, 1974.

[3] I. Horowitz and P. Rosenbaum, "Non-linear Design for Cost of Feedback Reduction in Systems with Large Parameter Uncertainty," *Int. J. Contr.*, vol. 21, pp. 977–1001, 1975.

[4] O. Beker, C. V. Hollot, and Y. Chait, "Fundamental Properties of Reset Control Systems," *Automatica*, vol. 40, pp. 905–915, 2004.

[5] R. H. Middleton, G. C. Goodwin, D. J. Hill, and D. Q. Mayne, "Design Issues in Adaptive Control," *IEEE Trans. Automatic Control*, vol. 33, pp. 50–58, 1988.

[6] P. V. Zhivoglyadov, R. H. Middleton, and M. Fu, "Localization Based Switching Adaptive Control for Time-varying Discrete-time Systems," *IEEE Trans. Automatic Control*, vol. 45, pp. 752–756, 2000.

[7] K. S. Narendra and J. Balakrishnan, "Improving Transient Response of Adaptive Control Systems Using Multiple Models and Switching," *IEEE Trans. Automatic Control*, vol. 39, pp. 1861–1866, 1994.

[8] K. S. Narendra and J. Balakrishnan, "Adaptive Control Using Multiple Models," *IEEE Trans. Automatic Control*, vol. 42, pp. 171–187, 1997.

[9] B. D. O. Anderson, T. Brinsmead, D. Liberzon, and S. Morse, "Multiple Model Adaptive Control with Safe Switching," *Int. J. Adapt. Control Signal Process.*, vol. 15, pp. 445–470, 2001.

[10] A. Cezayirli and K Ciliz, "Multiple Model Based Adaptive Control of a DC Motor under Load Changes," in *Proc. of Mechatronics, ICM '04*, Istanbul, Turkey, June 2004, pp. 328 – 333.

[11] J. Kalkkuhl, T. A. Johansen, J. Lüdemann, and A. Queda, "Nonlinear Adaptive Backstepping with Estimator Resetting Using Multiple Observers," in *Proc. Workshop on Hybrid Systems, Computation and Control, Rome*, 2001.

[12] L. Chen and K. S. Narendra, "Nonlinear Adaptive Control using Neural Networks and Multiple Models," *Automatica*, vol. 37, pp. 1245–1255, 2001.

[13] K. S. Narendra and K. George, "Adaptive Control of Simple Nonlinear Systems Using Multiple Models," *Proc. Amer. Contr. Conf.*, pp. 1779–1784, 2002.

[14] J. Kalkkuhl, T. A. Johansen, and J. Lüdemann, "Improved Transient Performance of Nonlinear Adaptive Backstepping Using Estimator Resetting Based on Multiple Models," *IEEE Transactions on Automatic Control*, vol. 47, pp. 136 –140, Jan 2002.

[15] D. Dougherty, J. Arbogast, and D. Cooper, "A Multiple Model Adaptive Control Strategy for DMC," in *Proc. Amer. Contr. Conf.*, Denver, Colorado, June 2003.

[16] B. Chaudhuri, R. Majumder, and B Pal, "Application of Multiple-Model Adaptive Control Strategy for Robust Damping of Interarea Oscillations in Power System," *IEEE Trans. on Control Systems Tech.*, vol. 12, no. 5, pp. 727–736, nov 2004.

[17] J. Bakkeheim and T. A. Johansen, "Transient Performance, Estimator Resetting and Filtering in Nonlinear Multiple Model Adaptive Backstepping Control," *IEE Proc.-Control Theory Appl.*, vol. 153, pp. 536–545, 2006.

[18] M. K. Ciliz and A. Cezayirli, "Increased Transient Performance for the Adaptive Control of Feedback Linearizable Systems Using Multiple Models," *Int. J. Contr.*, vol. 79, pp. 1205–1215, 2006.

[19] M. S. Branicky, "Multiple Lyapunov Functions and Other Analysis Tools for Switched and Hybrid Systems," *IEEE Transactions on Automatic Control*, vol. (43:4), pp. 475–482, April 1998.

[20] D. Radan, Ø. N. Smogeli, A. J. Sørensen, and A. K. Ådnanes, "Operating Criteria for Design of Power Management Systems on Ships," in *Proc. of the 7th IFAC Conference on Manoeuvring and Control of Marine Craft (MCMC'06)*, Lisbon, Portugal, 2006.

[21] Ø. N. Smogeli, J. Hansen, A. J. Sørensen, and T. A. Johansen, "Anti-spin Control for Marine Propulsion Systems," in *IEEE Conference on Decision and Control*, Bahamas, Dec. 2004.

[22] Ø. N. Smogeli, A. J. Sørensen, and K. J. Minsaas, "The Concept of Anti-spin Thruster Control," *Control Engineering Practice*, 2006, to appear.

[23] Ø. N. Smogeli and A. J. Sørensen, "Anti-spin Thruster Control for Ships," *Automatica*, 2006, submitted.

[24] Ø. N. Smogeli, *Control of Marine Propellers: from Normal to Extreme Conditions*, Ph.D. thesis, Department of Marine Technology, Norwegian University of Science and Technology (NTNU), 2006.

[25] J. Bakkeheim, Ø. N. Smogeli, T. A. Johansen, and A. J. Sørensen, "Improved Transient Performance by Lyapunov-based Integrator Reset of PI Thruster Control in Extreme Seas," in *IEEE Conference on Decision and Control*, San Diego, USA, 2006.

[26] M. Krstic, I. Kanellakopoulos, and P. Kokotovic, *Nonlinear and Adaptive Control Design*, John Wiley and sons, Inc, 1995.

[27] J. M. Maciejowski, *Predictive Control with Constraints*, Prentice-Hall, England, 2002.

[28] João Hespanha, "Hysteresis-based Switching Algorithms for Supervisory Control of Uncertain Systems," *Automatica*, vol. 39, pp. 263–272, 2003.

[29] A. J. Sørensen, "Structural Issues in the Design and Operation of Marine Control Systems," *IFAC Journal of Annual Reviews in Control*, vol. (29:1), pp. 125–149, 2005.

[30] T. I. Fossen, *Marine Control Systems*, Marine Cybernetics, 1 edition, 2002.

[31] H. K. Khalil, *Nonlinear Systems (3rd Ed.)*, Prentice-Hall, New York, 2001.

[32] Ø. N. Smogeli, A. J. Sørensen, and T. I. Fossen, "Design of a Hybrid Power/Torque Thruster Controller with Thrust Loss Estimation," in *Proc. IFAC Conference on Control Applications in Marine Systems (CAMS'04)*, Ancona, Italy, 2004.